

ACTUATOR CONSTRAINTS HANDLING IN HIGHER HARMONIC CONTROL ALGORITHMS FOR VIBRATION REDUCTION

R. M. Morales^{*◇}, M. C. Turner^{*}, P. Court[†] and C. Hutchin[†]

^{*} Dept. of Engineering, University of Leicester, University Rd., Leicester, UK, LE1 7RH, UK

[†] AgustaWestland Ltd., Yeovil, BA20 2YB, UK.

[◇] Corresponding author: rmm23@le.ac.uk

Abstract

This paper discusses the advantages of using quadratic-programming-based higher harmonic control (HHC) algorithms for vibration reduction applications. Their benefits when dealing with actuator constraints in comparison with scaling, truncation and weight manipulation of the control efforts have been exposed in previous works. The main contribution of this work is the discussion in more detail of important implementation aspects of the quadratic programming in the context of Higher Harmonic Control. Equivalent translations of flapping constraints via constraints of the Fourier coefficients are not always possible in a quadratic-programming framework and approximations of the feasible region are required. Such approximations should be taken into consideration carefully to avoid significant loss of optimal performance. The benefits of incorporating quadratic programming algorithms in the HHC design problem are shown for a linearised representation of a five-blade coupled rotor-fuselage model augmented with active trailing edge flaps.

1 INTRODUCTION

Vibrations form a very important aspect in the design and operation of rotorcraft vehicles. Current research and technology development efforts are devoted to mitigate the detrimental effects of vibrations since they contribute towards decreased airworthiness, mechanical wearing and decreased flight comfort. A major source of vibration in helicopters, which can be treated using control algorithms operating in steady conditions during forward flight, is originated from periodic forces and moments at the main rotor hub. A rotor with identical blades under identical loading and undergoing identical motion, the hub forces and moments are characterised by multiples of N/rev (N being the number of rotor blades), with the N/rev harmonic being the most dominant [5]. In turn, the vibrations at the rotor hub can be attributed to the complex wake structure, unsteady flow field and stall effects. Active rotor technologies are exploring the use of active elements in both the fixed and the rotating frame of the main rotor to produce the required actuating signals to mitigate the undesired vibrations. Under this scope, active trailing edge flaps (ATEFs), which are mounted on each rotor blade, represent a promising technology with the advantages of low power con-

sumption and conceptual simplicity [10].

The success of a control strategy relies heavily in the quality of the models of the process to control. Control theory offers well-established methods when essential features of the vibration process around well-known operating conditions can be captured by static or Linear-Time-Invariant (LTI) representations, expressed usually in the form of transfer function matrices or state-space representations [11]. Most control strategies for vibration reduction purposes are developed for such representations of the vibratory process. Static models can capture the multi-harmonic nonlinear behaviour [6] of the vibratory process [5] whereby an active element in the rotating frame operating at a certain frequency exerts an influence on other harmonics of the vibration at the rotor hub. Note however that static models imply that any control actions have an immediate effect on the hub vibrations, which assumes the transient characteristics of the process are insignificant. This assumption makes it more difficult to guarantee or predict reliably stability and performance levels even around some neighbourhood of the operating condition. On the other hand, LTI models can not capture such a multi-harmonic behaviour due to the superposition principle that governs LTI systems. However, they allow con-

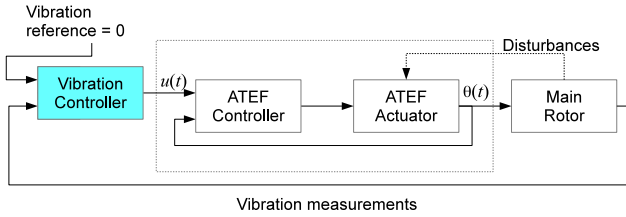


Figure 1: Overall control structure for vibration control using ATEF actuators.

ventional *feedback control* [11] methods to account for the transient behaviour of the vibratory process and hence offering more reliable predictions about the success of the control strategy. The main advantage of using adaptive or feedback control design methods in comparison to empirical approaches, is the guarantee of an optimised behaviour in ideal conditions given some prescribed performance demand and control authority. Overall, all control approaches using ATEF actuators can be represented by a two-layer control architecture, as shown in Figure 1. The vibration controller, which is the element of attention in this work, determines desired flapping signals $u(t)$ required to reduce vibrations. A second element, the actuator controller, has the goal of reproducing as closely as possible the flapping signals demanded by the vibration controller. The success of the overall vibration reduction system depends on the success of both the vibration and the ATEF controller systems.

A very well (perhaps the most) known control strategy to mitigate vibration is known as *Higher Harmonic Control* (HHC) [4]. The strategy is constructed from the assumption of a static linear relation between the Fourier coefficients of the most dominant harmonic of the vibrations and chosen (higher) harmonics of the actuation. Typically, the modelling assumption extends to the existence of a baseline vibration, which is a non-zero vibration in the presence of zero actuation. HHC methods developed under such static modelling assumptions can be categorised as *Adaptive Control* [1], since the controller gains are updated from regular estimations of the open-loop process. Typically, the control law is constructed from the solution of an *unconstrained optimisation problem* [2] such as Least Squares, whereby a performance function, which encapsulates a weighted combination between vibration energies and actuation efforts, is minimised.

ATEF actuators can only deliver a limited range of deflection angles. A common approach to deal with such constraints is to *scale* or *truncate* (clip) the control actions obtained from the solution of the unconstrained optimisation problem. Another approach is to manipulate the weight associated with control authority in the performance function until the constraints are

satisfied. Scaling and truncation can degrade significantly the achievable performance and such disadvantages have already been exposed in [3]. Weight manipulation has the problem that the process of choosing a priori the input weight to meet the flapping constraints is not transparent. Iterative weight manipulation can become computationally very expensive making it very difficult for real implementations [3]. In addition, overweighting control authority to ensure flapping constraints can lead to poor performance results.

To overcome the issues exposed by scaling, truncation and weight manipulation, constrained optimisation techniques have been explored and shown to be a successful alternative [3]. This paper pays particular attention to *Quadratic Programming* (QP) and shows its benefits over the the afore-mentioned techniques. The main contribution of this work is the discussion in more detail of important implementation aspects of the QP in the context of HHC algorithms for vibration reduction. Equivalent translations of flapping constraints via constraints of the Fourier coefficients are not always possible in a QP framework and approximations are required. Such approximations should be taken into consideration carefully to avoid significant loss of optimal performance.

The paper is structured as follows. Section 2 introduces the static model representation for the vibratory process and used in conventional HHC algorithms. Section 3 explains how to incorporate QP laws in the HHC problem and important implementation aspects of this control approach are discussed in section 4. The benefits of incorporating QP algorithms in the HHC design problem are shown in section 5 for a linearised representation of a five-blade coupled rotor-fuselage model augmented with active trailing edge flaps operating at cruise flying conditions. The work concludes with some final remarks in section 6.

2 Conventional HHC

HHC is constructed from the assumption that the relation between the Fourier (sine and cosine) coefficients of the input and output forces and moments [4] is linear. Define a vector y_k as the output containing the harmonics of the loads and vibrations at the time instant indicated via the index k , with $t = k\Delta t$ and Δt representing the time gap between each implementation of the control actions. Likewise, define the input vector u_k containing the harmonics of a control input signal. The above assumption in the modelling of the rotor system is encapsulated in the following mathematical expression:

$$(1) \quad y_k = Tu_k + d$$

where d represents the harmonics of the baseline vibration, which is equivalent to y_k when the control inputs are zero ($u_k = 0$). Commonly, the matrix T is referred to as the *interaction matrix* or *sensitivity matrix* [8]. The above model is referred by Johnson [4] as the *global model* of helicopter response and can be rewritten as

$$(2) \quad y_k = y_0 + T(u_k - u_0)$$

This model implies that both the interaction matrix T and d are time-invariant and any change in the control input will have an immediate effect on the output vibration. Also, u_0 represents the control action required to trim the rotor and sets the initial control input for subsequent control actions.

Typically, control algorithms developed for static and quasi-static models are based on the minimisation of a performance function J_k at the index time k , which is expressed in a quadratic form for mathematical convenience, and whereby a trade-off between vibration reduction and actuator authority is specified:

$$(3) \quad u_k^\dagger = \arg \min_{u_k} \underbrace{y_k^T Q y_k + u_k^T R u_k}_{J_k}$$

Typically, y_k contains the sine and cosine components of the N/rev fixed hub loads and moments: $F_x, F_y, F_z, M_x, M_y,$ and M_z . Control actuation corresponds to the Fourier coefficients of the actuator signals, usually at $N - 1, N$ and $(N + 1)/\text{rev}$. The weight $Q = Q^T > 0$ is used to target specific vibration reduction among some of the vibration channels. Likewise, the weight $R = R^T > 0$ is used to specify actuator authority. Often, both weights are diagonal and may be scaled differently if sensor measurements are provided in different units. A good starting point when designing the controller is to choose the same weight (given that all vibration and load measurements as well as actuator signals are provided in the same units) for all channels, which corresponds to $Q = R = I$. The above optimisation problem can be solved analytically by making

$$(4) \quad \frac{\partial J_k}{\partial u_k} = 0$$

Solving for u_k provides the following analytical expression for the optimal control input

$$(5) \quad u_k^\dagger = -(T^T Q T + R)^{-1} (T^T Q) \underbrace{(y_0 - T u_0)}_d$$

3 HIGHER HARMONIC CONTROL via QP

The implementation of unconstrained control laws can lead to actuation signals which exceeds actuator limits. In terms of simultaneous reduction of vibration

and noise [9], the drawbacks of using scaling and truncation of the control inputs can be clearly noticed by significant increases of vibration and noise measurements with respect to the optimal performance, see for instance [3]. Another approach is to manipulate the weight R associated with the control input, but it has the risks of demanding large computational efforts [3] or overweighting the control actions and thus leading to poor performance results. Such issues will be illustrated clearly in the simulation results in Section 5. In order to better handle actuator constraints, it is recommended to use instead optimisation algorithms which minimise the performance function given a *feasible* set of control input values. If the objective function is (convex) quadratic and the constraint functions are linear inequalities equalities, the control algorithm can be implemented as a *Quadratic Programming* [2]:

$$(6) \quad \begin{aligned} u_k^\dagger &= \arg \min_{u_k} \underbrace{y_k^T Q y_k + u_k^T R u_k}_{J_k} \\ \text{s.t.} \quad & H u_k \leq f \end{aligned}$$

The above constrained optimisation problem can be equivalently written only in terms of the optimisation variable u_k with the use of (1) as:

$$(7) \quad \begin{aligned} u_k^\dagger &= \arg \min_{u_k} \frac{1}{2} u_k^T (T^T Q T + R) u_k + u_k^T T^T Q d \\ \text{s.t.} \quad & H u_k \leq f \end{aligned}$$

Note that the symbol \leq indicate element-wise inequality. If the vector u_k has dimension q and the numbers of inequalities requires to express the flapping constraints is p , then H and f have dimensions $p \times q$ and $p \times 1$, respectively. A region of actuator signals is specified via the polyhedron $H u_k \leq f$. Such a polyhedron can be sufficient to specify feasible actuation signals for active rotor applications (more general feasible regions in convex optimisation problems include also solution sets of equality constraints which are affine). Polyhedral regions of such a form are defined as the solution set of a finite number of linear inequalities, or equivalently, the intersection of a finite number of half spaces [2].

4 IMPLEMENTATION OF QP-BASED HHC

It is argued that the solution of convex optimisation problems via interior-point methods works very well in practice [2]. They can solve the problem in a number of steps or interactions that is almost always in the range between 10 and 100. In general, each step requires on the order of $\max\{q^3, q^2 p, F\}$ operations; with F denoting the cost of evaluating the first and second derivatives of the objective and constraint

functions. q is the dimension of the optimisation variable u_k and p represent the number of inequality constraints.

Another important aspect to consider is that of expressing min-max actuation signals via polyhedra regions, which can introduce some performance limitations of the QP. To visualise this aspect, consider for instance having one ATEF actuator per blade operating at a single frequency n/rev :

$$(8) \quad u(t) = u_{c,n} \cos(n\Omega t) + u_{s,n} \sin(n\Omega t) + u_0$$

The flapping constraint is typically expressed

$$(9) \quad |u(t)| \leq \bar{u}, \forall t$$

The above inequality can be written equivalently as

$$(10) \quad \begin{aligned} |u_0| &\leq \bar{u} \\ u_{c,n}^2 + u_{s,n}^2 &\leq (\bar{u} - |u_0|)^2 \end{aligned}$$

for some positive \bar{u} . The above flapping constraint can not be expressed clearly via linear inequality constraints due to the quadratic terms. A common approach to overcome this issue is to use *box constraints* instead so for each control input we have:

$$(11) \quad \begin{aligned} |u_0| &\leq k\bar{u} \\ |u_{c,n}| &\leq k\bar{u} \\ |u_{s,n}| &\leq k\bar{u} \end{aligned}$$

with the positive scaling factor k adjusted with the smallest values so the box is just contained within the true flapping constraint region. For instance, if u_0 was fixed to be zero, then $k = 1/\sqrt{2}$ is the factor so the box constraints (a square region) just fits within the feasible (circle) region. Another alternative is to use more sophisticated linear constraints to better represent the true flapping constraints, such as

$$(12) \quad \begin{aligned} |u_0| &< \bar{u} \\ |u_{c,n}| + |u_{s,n}| &\leq \bar{u} - |u_0| \end{aligned}$$

Graphically, the above flapping constraints translate in approximating the conic region (10) into box (11) or pyramidal constraints (12) and hence leading to less conservative results, see Figure 2.

4.1 General approximation of flapping constraints via ‘‘pyramidal’’ regions

In general, let the ATEF signals be expressed in the time-domain as

$$\begin{aligned} u_i(t) &= u_{i,0} + \sum_{n=\underline{n}}^{\bar{n}} (u_{i,c,n} \cos(n\Omega t) + u_{i,s,n} \sin(n\Omega t)) \\ &= u_{i,0} + \sum_{n=\underline{n}}^{\bar{n}} \sqrt{u_{i,c,n}^2 + u_{i,s,n}^2} \\ &\quad \cos\left(n\Omega t + \arctan\left(\frac{u_{i,s,n}}{u_{i,c,n}}\right)\right) \end{aligned}$$

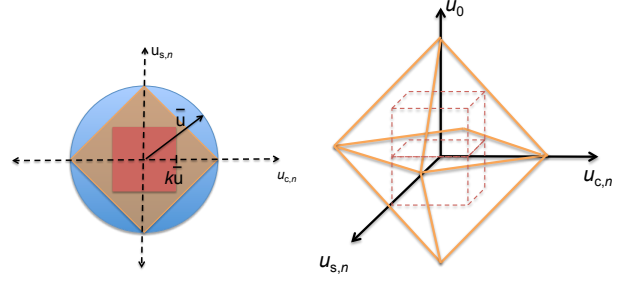


Figure 2: *Left*: Top view of the feasible flapping conic region (10) and two approximations: box (11) and pyramidal (12) constraints. *Right*: three-dimensional representation of the approximation regions.

The index triad $\{i, \{c, s\}, n\}$ is used to easily map the harmonic coefficients. The first index $i = \{1, \dots, \bar{i}\}$ has been included to account for the fact that there can be more than one actuator on each blade. It is common to find two ATEFs with one actuator mounted in the *inboard* and the other on the *outboard* section of the blade to increase control power. The second index set $\{c, s\}$ are include to indicate the cosine and sine coefficients. The index $n = \{\underline{n}, \underline{n} + 1, \dots, \bar{n}\}$ denotes the frequency multiples at which the actuator operates.

Flapping constraints are expressed for each actuator as

$$(13) \quad |u_i(t)| < \bar{u}, \forall i, t$$

Such constraints can be equivalently expressed as

$$\begin{aligned} |u_{i,0}| &< \bar{u}, \forall i \\ \sum_{n=\underline{n}}^{\bar{n}} \sqrt{u_{i,c,n}^2 + u_{i,s,n}^2} &\leq \bar{u} - |u_{i,0}|, \forall i \end{aligned}$$

‘‘Pyramidal’’ approximations to the above flapping constraint can be expressed as

$$(14) \quad \begin{aligned} |u_{i,0}| &< \bar{u}, \forall i \\ \sum_{n=\underline{n}}^{\bar{n}} |u_{i,c,n}| + |u_{i,s,n}| &\leq \bar{u} - |u_{i,0}|, \forall i \end{aligned}$$

which can be clearly implemented via linear inequalities.

4.2 Alternative implementations of QP-based HHC for vibration reduction

In terms of the implementation of the QP, the above possibilities of representing non-polyhedral flapping constraints via polyhedral methods, open the question about what method is appropriate to implement the constrained optimisation algorithms in a non-conservative way yet effectively, i.e., with affordable computational efforts.

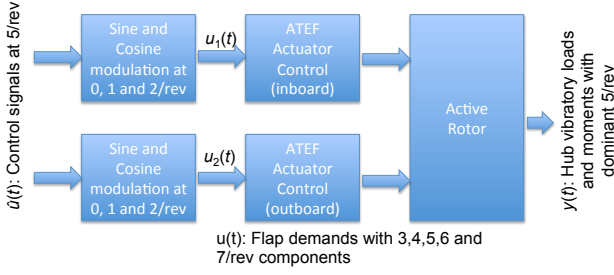


Figure 3: Schematic of the open-loop system.

The use of improved approximations to represent the original feasible region more accurately is perhaps the most recommendable approach but care must be taken not to use an unnecessary high number of linear inequality constraints and avoid very large design efforts.

Scaled box constraints are the easiest to specify but they could yield very conservative performance, see Figure 2. To improve over this aspect, an alternative is to iterate over the scaling factor of the “box” as follows:

- i) Adjust the scaling factor k so the flapping constraint set is just contained.
- ii) Solve the QP and evaluate whether the optimal solution is feasible.
- iii) If yes, then implement control action.
- iv) If no, reduce the scaling factor k and go to ii).

It is clear that once the scaling factor is reduced by a certain value so the scaled box is inside the flapping constraint region, the obtained solution is feasible. In other words, the algorithm is guaranteed to converge to a solution in a finite number of steps. The maximum number of steps are determined by the size of the decrements in step iv). In the end and given the specific application, the designer should decide by carrying out preliminary studies via simulations with computer models on the approaches presented earlier (approximation of flap constraints or iterative box constraints) according to a desired trade-off between speed and performance.

5 SIMULATIONS

In order to illustrate the ideas discussed in this report, simulations have been performed on linearised model of a coupled-rotor fuselage model (CRFM) augmented with ATEF actuators for vibration reduction purposes. The rotor has $N = 5$ blades and two active trailing edge actuators mounted on each blade: inboard ($i = 1$) and outboard ($i = 2$). In order to obtain a linear model, the CRFM has been linearised around

a given cruise flight condition. With this purpose, manipulated amplitude and phase (or cosine and sine coefficients) of 5/rev harmonics are chosen as control signals. Rotor theory explains that forces and moments in the rotating frame at 3, 4, 5, 6 and 7/rev will have a significant influence on the 5/rev component of the vibratory loads and moments, which are the desired signals to be controlled [5]. In order to produce flapping signals with such frequency components, the 5/rev inputs are modulated with 0, 1 and 2 /rev harmonics, see Figure 3. For simplicity, we will assume ideal actuation, i.e., the delivered and demanded flapping signals are the same.

To consider the modulation in more detail, the control signals are chosen as follows:

$$\hat{u}(t) = \begin{bmatrix} \hat{u}_{1,c} \\ \hat{u}_{2,c} \\ \vdots \\ \hat{u}_{10,c} \end{bmatrix} \cos(5\Omega t) + \begin{bmatrix} \hat{u}_{1,s} \\ \hat{u}_{2,s} \\ \vdots \\ \hat{u}_{10,s} \end{bmatrix} \sin(5\Omega t)$$

with all cosine and sine coefficients being the elements of the vector u_k . Modulation with lower (0, 1 and 2/rev) harmonics and following the structure of the control inputs provided by CRFM, the following flapping signal for the inboard actuator is produced

$$\begin{aligned} u_1(t) = & (\hat{u}_{1,c} \cos(5\Omega t) + \hat{u}_{1,s} \sin(5\Omega t)) + \\ & (\hat{u}_{3,c} \cos(5\Omega t) + \hat{u}_{3,s} \sin(5\Omega t)) \cos(\Omega t) + \\ & (\hat{u}_{5,c} \cos(5\Omega t) + \hat{u}_{5,s} \sin(5\Omega t)) \sin(\Omega t) + \\ & (\hat{u}_{7,c} \cos(5\Omega t) + \hat{u}_{7,s} \sin(5\Omega t)) \cos(2\Omega t) + \\ & (\hat{u}_{9,c} \cos(5\Omega t) + \hat{u}_{9,s} \sin(5\Omega t)) \sin(2\Omega t) \end{aligned}$$

Simplifying the above expression by the use of trigonometric identities, we obtain that

$$u_1(t) = \sum_{n=3}^7 (u_{1,c,n} \cos(n\Omega t) + u_{1,s,n} \sin(n\Omega t))$$

where

$$\begin{aligned} u_{1,c,3} &= \frac{1}{2}(\hat{u}_{7,c} + \hat{u}_{9,s}), & u_{1,s,3} &= \frac{1}{2}(\hat{u}_{7,s} - \hat{u}_{9,c}) \\ u_{1,c,4} &= \frac{1}{2}(\hat{u}_{3,c} + \hat{u}_{5,s}), & u_{1,s,4} &= \frac{1}{2}(\hat{u}_{3,s} - \hat{u}_{5,c}) \\ u_{1,c,5} &= \hat{u}_{1,c}, & u_{1,s,5} &= \hat{u}_{1,s} \\ u_{1,c,6} &= \frac{1}{2}(\hat{u}_{3,c} - \hat{u}_{5,s}), & u_{1,s,6} &= \frac{1}{2}(\hat{u}_{3,s} + \hat{u}_{5,c}) \\ u_{1,c,7} &= \frac{1}{2}(\hat{u}_{7,c} - \hat{u}_{9,s}), & u_{1,s,7} &= \frac{1}{2}(\hat{u}_{7,s} + \hat{u}_{9,c}) \end{aligned}$$

A similar simplification can be done for the outboard flapping:

$$u_2(t) = \sum_{n=3}^7 (u_{2,c,n} \cos(n\Omega t) + u_{2,s,n} \sin(n\Omega t))$$

where

$$\begin{aligned}
u_{2,c,3} &= \frac{1}{2}(\hat{u}_{8,c} + \hat{u}_{10,s}), & u_{2,s,3} &= \frac{1}{2}(\hat{u}_{8,s} - \hat{u}_{10,c}) \\
u_{2,c,4} &= \frac{1}{2}(\hat{u}_{4,c} + \hat{u}_{6,s}), & u_{2,s,4} &= \frac{1}{2}(\hat{u}_{4,s} - \hat{u}_{6,c}) \\
u_{2,c,5} &= \hat{u}_{2,c}, & u_{2,s,5} &= \hat{u}_{2,s} \\
u_{2,c,6} &= \frac{1}{2}(\hat{u}_{4,c} - \hat{u}_{6,s}), & u_{2,s,6} &= \frac{1}{2}(\hat{u}_{4,s} + \hat{u}_{6,c}) \\
u_{2,c,7} &= \frac{1}{2}(\hat{u}_{8,c} - \hat{u}_{10,s}), & u_{2,s,7} &= \frac{1}{2}(\hat{u}_{8,s} + \hat{u}_{10,c})
\end{aligned}$$

Let the behaviour of the system at a given cruise condition be captured by a LTI transfer function matrix $G(s)$, see [11]. The linear representation of the CRFM at a given rotor speed Ω can be obtained then by the complex matrix $G(j\Omega)$. The vibratory response in the frequency domain with 5/rev ATEF inputs is in the form of (1) with

$$T = \begin{bmatrix} \operatorname{Re}\{G(j5\Omega)\} & \operatorname{Im}\{G(j5\Omega)\} \\ -\operatorname{Im}\{G(j5\Omega)\} & \operatorname{Re}\{G(j5\Omega)\} \end{bmatrix}$$

with $u_k = [\hat{u}_{1,c}, \dots, \hat{u}_{10,c}, \hat{u}_{1,s}, \dots, \hat{u}_{10,s}]^T$. If the j -th channel of the vibration signal is expressed as (15)

$$y_i(t) = y_{j,0} + \sum_{n=1}^{\infty} (y_{i,c,n} \cos(n\Omega t) + y_{i,s,n} \sin(n\Omega t))$$

then $y_k = [y_{1,c,5}, \dots, y_{6,c,5}, y_{1,s,5}, \dots, y_{6,s,5}]^T$. The upper and lower blocks of the baseline vibration d contain the cosine and sine Fourier coefficients of the 5/rev vibration harmonic with zero flapping, respectively.

The exact translation of flapping constraints for both actuators in terms of the sine and cosine Fourier coefficients is not straightforward. For the sake of simplicity and economic design efforts, we first explore if box constraints lead to satisfactory results:

$$\begin{aligned}
|\hat{u}_{j,c,n}| &\leq k\bar{u} \\
|\hat{u}_{j,s,n}| &\leq k\bar{u}
\end{aligned}$$

Flapping constraints are given with $\bar{u} = 1$ and we chose $k = 0.37$ to guarantee the flapping constraints. The simulation results performed with the linear representation are shown in Figures 4 and 5. In order to emphasise the importance of handling appropriately the constraints, we have compared the vibration results with the practice of scaling, truncation and overweighting. It is clearly seen from Figure 4 the significant performance degradation when using scaling and truncation of the control inputs. Further remarks follow below:

- The results obtained with the QP are very successful in the sense that they are not too different with respect to the optimal case (unconstrained optimisation): all vibration reduction levels are

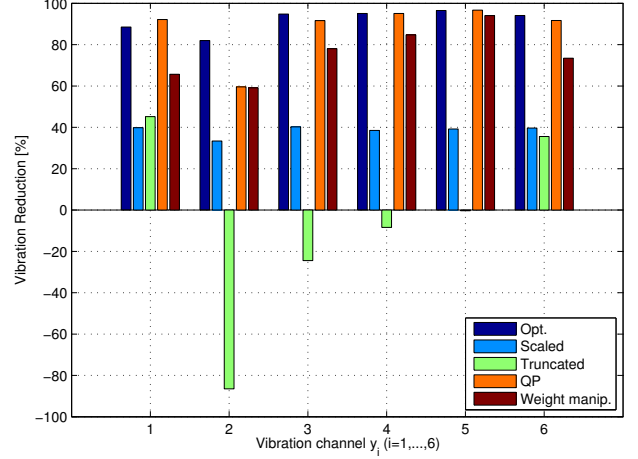


Figure 4: Achieved vibration results.

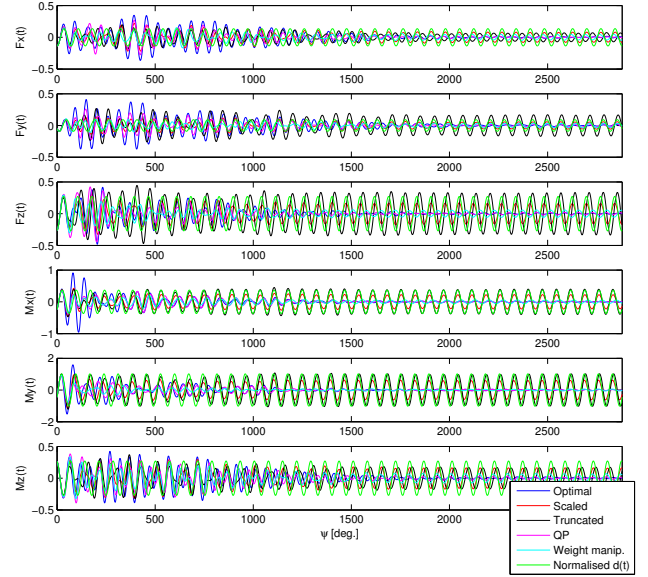


Figure 5: Normalised Vibration signals.

very similar in all vibration channels except in the in-plane horizontal component $F_y(t)$ whereby a decrease of about 20% in vibration reduction is observed.

- It is corroborated in this simulation study the deterioration in performance produced by the use of scaling and truncation. Truncation was found to be much worse than scaling producing a significant increase in vibration in $F_y(t)$. Scaling provides in average a loss of about 50% in vibration reduction with respect to the optimal case. Vibrations in $F_z(t)$ and $M_x(t)$ were increased also by the use of truncation.
- The degradations by overweighting are less severe than scaling and truncation. Simulations show the worst degradation occurring in $F_y(t)$.

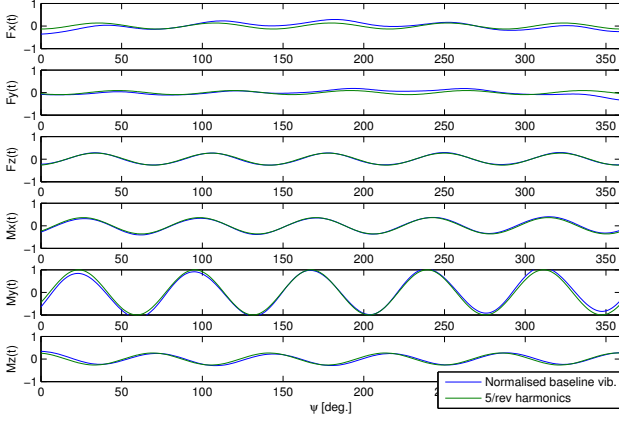


Figure 6: Normalised Baseline vibration.

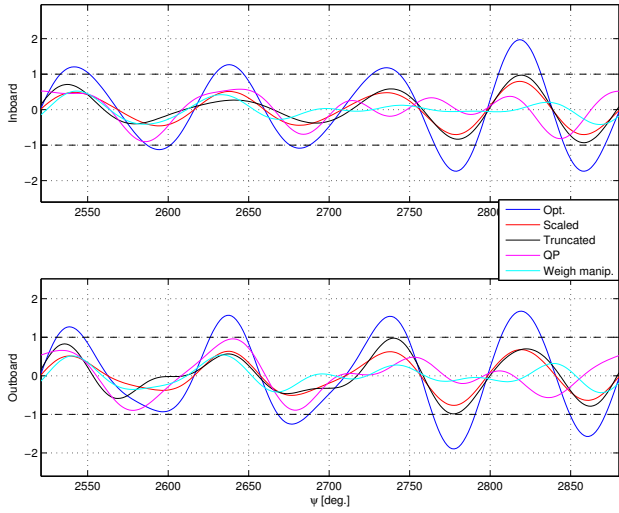


Figure 7: Normalised desired actuator signals.

Overall, overweighting underperforms the QP-based algorithms in all vibration channels.

- Despite the use of box constraints in the QP, the obtained performance is not too compromised, suggesting that for this particular case the approximation via box constraints is satisfactory. Recall that the use of box constraints simplifies significantly the efforts when compared to more sophisticated approximations. The QP was executed in Matlab and it takes about 25 iterations and 0.03 seconds to solve the QP problem with a 2.66 GHZ Intel core 2 duo.
- If $\|\hat{u}(\omega)\| > k_s \bar{u}$ then scaling is performed as

$$(16) \quad \hat{u}_s(\omega) = \frac{\hat{u}(\omega)^\dagger}{\|\hat{u}(\omega)^\dagger\|} k_s \bar{u}$$

with the complex vector $\hat{u}(\omega)^\dagger$ being the phasor representation of $\hat{u}(t)$ with the Fourier coefficients obtained from the unconstrained optimisa-

tion problem. The scaling factor $k_s = 1$ was adjusted to guarantee the min-max flap constraints.

- Truncation is performed on a channel-basis. Let the i -th component of $\hat{u}(\omega)$ be denoted by $\hat{u}_i(\omega)$. If $\|\hat{u}_i(\omega)^\dagger\| > k_t \bar{u}$, then

$$(17) \quad \hat{u}_{t_i}(\omega) = \frac{\hat{u}_i(\omega)^\dagger}{\|\hat{u}_i(\omega)^\dagger\|} k_t \bar{u}$$

for all channels i . Again, the scaling factor $k_t = 0.55$ was adjusted to guarantee the min-max flap constraints.

- The control effort weight R was increased by a factor of 5×10^4 in the “weight manipulation” scenario with respect to the value used in the unconstrained optimisation problem to ensure the min-max flap constraints.

Figure 6 shows that the baseline vibration has a 5/rev dominant component. Normalised flapping signals for all considered control methods are shown in the time domain in Figure 7.

6 CONCLUDING REMARKS

This work has been focused on control strategies for vibration reduction using static models. Actuator limitations can impose significant limitations to the achievable performance and they must be treated carefully. We have paid particular attention to Quadratic Programming (QP) and their benefits over clipping, scaling and weight manipulation methods to deal appropriately with actuator constraints. We discussed also alternative ways of implementing QP-based algorithms to account for any conservatism introduced by approximating actuator limitations in Higher Harmonic Control problems, which are generally non-linear, via linear matrix inequalities. Simulation results show clearly the significant benefits of the QP approach, the possibility of using non-sophisticated approximation regions for actuator constraints and the dangers of mishandling them. Simulations assumed ideal actuation, however, actuator dynamics can restrict the achievable performance and the designer should take this into account when implementing HHC systems for vibration reduction in real applications. The constraint handling methods considered in this report might be complemented with advanced actuator control design methods, such as anti-windup [7], to improve actuator response and therefore the overall performance.

ACKNOWLEDGEMENTS

This work was performed as part of the Rotorcraft Technology Validation Programme, and support from

the UK Technology Strategy Board is gratefully acknowledged.

COPYRIGHT STATEMENT

The authors confirm that they, and/or their company or organisation, hold copyright on all of the original material included in this paper. The authors also confirm that they have obtained permission, from the copyright holder of any third party material included in this paper, to publish it as part of their paper. The authors confirm that they give permission, or have obtained permission from the copyright holder of this paper, for the publication and distribution of this paper as part of the ERF2014 proceedings or as individual offprints from the proceedings and for inclusion in a freely accessible web-based repository.

References

- [1] K. Åström and B. Wittenmark. *Adaptive Control*. Dover Publications, 2008.
- [2] S. Boyd and L. Vandenberghe. *Convex Optimization*. Cambridge university press, 2004.
- [3] P. P. Friedmann and A. K. Padthe. Vibration and noise alleviation in rotorcraft using on-blade control implemented by microflaps. In *Proceedings of the 38th European Rotorcraft Forum*, Amsterdam, Netherlands, 2012.
- [4] W. Johnson. Self-tuning regulators for multicyclic control of helicopter vibration. Technical report, NASA, 1982.
- [5] W. Johnson. *Helicopter Theory*. Dover Publications, 1994.
- [6] H. K. Khalil. *Nonlinear Systems (third edition)*. Prentice Hall, Upper Saddle River, 2002.
- [7] R. M. Morales and M. C. Turner. Robust anti-windup design for active trailing edge flaps in active rotor applications. In *Proceedings of the 70th American Helicopter Society Forum*, Montreal, Canada, 2014.
- [8] D. Patt, J. Chandrasekar, D. S. Bernstein, and P. P. Friedmann. HHC algorithm for helicopter vibration reduction revisited. *Journal of Guidance, Control and Dynamics*, 28(5):918 – 930, 2005.
- [9] D. Patt, L. Liu, and P. P. Friedmann. Simultaneous vibration and noise reduction in rotorcraft using aeroelastic simulation. *Journal of the American Helicopter Society*, 51(2), 2006.
- [10] K. Ravichandran, I. Chopra, B. Wake, and B. Hein. Trailing-edge flaps for rotor performance enhancement and vibration reduction. *Journal of the American Helicopter Society*, 58(2):1–13(13), 2013.
- [11] S. Skogestad and I. Postlethwaite. *Multivariable Feedback Control: Analysis and Design (second edition)*. John Wiley & Sons, 2005.